PRELIMINARY RESULTS OF ULTRAVIOLET PHOTOMETRY OF SHELL STARS

Robert L. Bottemiller
University of Wisconsin
Madison, Wisconsin

ABSTRACT

Photometry of 40 B stars acquired by the OAO-2 has been examined for systematic differences between the 25 standard stars and 15 program objects. The latter include shell and Be stars and a few objects with at least a modest infrared excess. Although individual deviations did occur, no definite distinction between the program and comparison stars was found. A possible, but very weak, tendency for the program objects to lie somewhat below the standards in color-color plots is discussed, especially with reference to errors of misclassification and variability of the ultraviolet reddening law.

I. INTRODUCTION

Be stars, and the shell star sub-species, are differentiated from normal B-type stars in the visual region by line phenomena. Conversely, line emission and rotational effects, if they are significant, do not serve to separate these objects from the conventional early-type stars in color-color plots generated from UBV data.

However, modifications of the continuous flux distribution do occur in the ultraviolet for some objects. A previous paper in this volume by Coyne showed the emission in the Balmer continuum observed for γ Cas. OAO spectral scans of several other objects have displayed signs of similar behavior. Ground-based observations by Boone (1970) have also shown the tendency of Be stars to fill in the Balmer jump, occasionally to the

point of exhibiting a higher continuum level shortward of the Balmer limit. Other influences on the ultraviolet continuum of unproven importance are rotation (Collins and Harrington 1966) and the conversion of ultraviolet radiation into the infrared region by grains (Huang 1969).

With a considerable body of observational material available from the OAO, it is now possible to examine not only many normal early-type stars but also a number of Be and shell stars in the ultraviolet. The available OAO photometry provides a larger sample of shell star data than does the scanner material and also can be corrected for interstellar reddening in a straightforward manner.

The following paragraphs present the results of a comparison between normal, early-type and a sample of Be and shell stars in the form of reddening-corrected color-color plots based on OAO photometry. Errors in classification and in the application of the ultraviolet reddening curve are discussed in relation to these plots.

II. DATA REDUCTION

Ultraviolet magnitudes in five bandpasses were derived for 15 program and 25 standard stars. MK spectral types, V magnitudes and (B-V) indices were obtained from Lesh (1968) or Hiltner, Garrison and Schild (1969) with the exception of four standard and two program stars. For each object an unreddened $(B-V)_o$ value was assigned according to spectral type by means of Johnson's (1958) calibration.

A comparison of 12 program star spectral types determined spectroscopically with those found by the Q-method showed good agreement. With a single exception, the agreement was within one and a half spectral sub-types, or within about 0.03 units in (B-V). The one maverick, σ Cyg, is generally listed as B9 Iab but appears on a $(U-B)_o$-$(B-V)_o$ plot as slightly earlier than B5.

The magnitudes derived from data taken through the various OAO filters are denoted by the approximate effective wavelength for a specific filter; thus, the index $(m_{3320}-V)$ is written as (3320-V). With an estimate of E(B-V) in hand, the associated excess in $(\lambda-V)$ was computed using the mean $E(\lambda-V)/E(B-V)$ relation of Bless and Savage presented elsewhere in this volume. The interstellar reddening relation is highly non-linear in this wavelength region, besides being variable in direction. This difficulty together with uncertainties in $(B-V)_o$ and, hence, E(B-V) comprise the largest source of error in the computations.

The program stars were chosen on the following basis of decreasing desirability: i) shell stars, ii) Be stars, preferably with some indication of an infrared excess, and iii) ordi-

nary B stars with a known infrared excess. When the candidates were narrowed to those non-variable objects with satisfactory photometry, 15 stars remained. However, the OAO observing list has not been completely exhausted of interesting objects in this category, especially those with scans but little photometry and objects earlier than B1.

Table 1a lists the program stars, their MK types, V, B-V and indicates if the object has a noticeable infrared excess (with a reference) or a shell spectrum. Also tabulated are the ultraviolet magnitudes which form the basis for the reddening-corrected plots of $(\lambda-V)_o$ versus $(B-V)_o$.

The 25 standard stars (see Table 1b) span the spectral region from B0 to B9. Four of the latest types not classified by either Lesh or Hiltner, Garrison and Schild were assigned MK types from the Bright Star Catalog. The average E(B-V) for this sample is 0.05, with six objects having an excess greater than 0.10. The mean excess for 14 of the program stars, neglecting P Cygni's large excess, is 0.08. Including P Cygni raises the average excess to 0.12.

III. RESULTS

Color differences corrected for reddening, $(\lambda-V)_o$, were computed for all the program and comparison stars and plotted against $(B-V)_o$ for each of five ultraviolet filters. The results are all rather similar so graphs for only three bandpasses are presented in Figures 1a, b and c.

As one would expect, the normal B stars (filled circles) form well-defined sequences in these plots. A slight downturn at B9 in some filters may be due in part to minor misclassification and in part to observational inaccuracy. In any event, more standards of type B5 and later are desirable to solidify the definition of the sequence in this region.

A straight-line relation of the form $(\lambda-V)_o = m(B-V)_o + b$ was hand-fit to the data in a very approximate manner. The coefficients of slope, m, and intercept, b, are listed in Table 2 for all five filters.

The inverse relationship between slope and wavelength found in Table 2 naturally reflects the more rapid increase of flux in the near-to-far ultraviolet for stars in this spectral (temperature) range.

The small figure in the lower left corner of the first 3 plots represents the corrections to be made to the position of any given data point if it were assigned an incorrect $(B-V)_o$ or extinction ratio. If an object were misclassified so as to yield a $(B-V)_o$ too large or small by 0.02 units, its corrected horizontal displacement would be just that amount. In addition, a slight vertical correction would be necessary due to

Table 1a. Program Stars

Name/HD	MK	V	B-V	IR Excess?	Shell?	Ultraviolet Magnitudes 3320	2990	2390	2040	1680
P Cyg	B1 p	4.78	+0.41	Yes (1,2)	Yes	-1.76	-1.73	-1.05	-0.78	----
60 Cyg	B1 Vn	5.41	-0.20	---	No	-2.22	-2.61	-3.31	-3.65	-4.20
ω Ori	B2 IIIe$_1$	4.58	-0.11	Small (1)	No	-2.91	-3.23	-3.76	-3.88	-4.20
μ Cen	B2 IV-Ve$_3$	3.26	-0.16	---	No	-4.02	-4.40	-5.15	-5.53	-6.01
υ Cyg	B2 Ve$_{1+}$	4.28	-0.08	---	No	-2.96	-3.26	-3.78	-4.08	-4.47
ξ Cas	B2.5 V	4.81	-0.11	Small (1)	No	-2.30	-2.57	-3.00	-3.33	-3.85
ε Cas	B3 Vp	3.37	-0.16	No (1)	Yes	-3.78	-4.13	-4.62	-4.93	-5.24
217050	B4 IIIpe$_1$	5.42	-0.09	---	Yes	-1.44	-1.73	-2.11	-2.56	-2.95
ζ Tau	B4 IIIp	2.95	-0.19	---	Yes	-4.32	-4.67	-5.33	-5.42	-5.88
48 Lib	B5 IIIp	4.87	-0.10	Yes (2)	Yes	-2.16	-2.43	-2.74	-3.06	-3.55
ο And	B6 p	3.62	-0.09	---	Yes	-3.30	-3.55	-3.93	-4.27	-4.63
κ Dra	B6 IIIp	3.82	-0.11	Yes (1,2)	Yes	-3.25	-3.52	-4.02	-4.23	-4.44
23 Tau	B6 IV	4.18	-0.06	Small (1)	No	-2.67	-2.90	-3.35	-3.58	-3.89
η Tau	B7 III	2.87	-0.09	Small (1)	No	-3.84	-4.04	-4.48	-4.72	-5.15
σ Cyg	B9 Iab	4.23	+0.13	Small (1)	No	-2.21	-2.20	-1.92	-2.22	-2.50

[1]Johnson (1967), [2]Geisel (1970)

Table 1b. Standard Stars

Name/HD	MK	V	B-V	Ultraviolet Magnitudes 3320	2990	2390	2040	1680
69 Cyg	B0 Ib	5.94	-0.10	-1.67	-1.99	-2.50	-2.66	-3.17
τ Sco	B0 V	2.82	-0.25	-4.99	-5.35	-6.18	-6.69	-7.31
υ Ori	B0 V	4.61	-0.28	-3.25	-3.74	-4.53	-5.03	-5.44
δ Sco	B0.5 IV	2.30	-0.11	---	---	---	---	-7.08
ϕ^1 Ori	B0.5 IV-V	4.41	-0.17	-3.23	-3.62	-4.23	-4.58	-4.98
23 Ori	B1 Vn	4.99	-0.15	-2.59	-2.95	-3.47	-3.83	-4.23
ω^1 Sco	B1 V	3.96	-0.04	-3.40	-3.69	-3.99	-4.33	-5.01
148703	B2 III	4.22	-0.17	-3.24	-3.62	-4.24	-4.55	---
φ Cen	B2 IV	3.82	-0.22	-3.76	-4.15	-4.90	-5.26	-5.76
ρ Sco	B2 IV-V	3.88	-0.20	-3.71	-4.11	-4.69	-5.02	-5.63
υ^1 Cen	B2 IV-V	3.86	-0.21	-3.63	-4.03	-4.82	-5.20	-5.70
22 Sco	B2 V	4.78	-0.12	-2.58	-2.94	-3.50	-3.81	-4.42
χ Cen	B2 V	4.35	-0.20	-3.14	-3.52	-4.24	-4.60	-5.13
129116	B3 V	3.99	-0.18	-3.41	-3.78	-4.4	-4.71	-5.19
125823	B3 V	4.41	-0.19	-3.06	-3.44	-4.07	-4.36	-4.89
λ Cru	B4 Vn	4.62	-0.16	-2.59	-2.94	-3.51	-3.82	-4.43
ϕ^2 Lup	B4 V	4.53	-0.16	-2.81	-3.14	---	-4.03	-4.40
137432	B4 Vp	5.42	-0.15	-1.80	-2.08	-2.63	-3.13	-3.47
ν And	B5 V	4.57	-0.16	-2.65	-2.98	-3.48	-3.76	-4.09
143699	B6 IV	4.88	-0.15	-2.35	-2.62	-3.09	-3.39	-3.80
144661	B7 IIIp	6.32	-0.06	-0.58	-0.81	-1.24	-1.39	-1.42
α Scl	B8 III	4.30	-0.16	-2.68	-2.94	-3.38	-3.76	-3.96
20 Tau	B8 III	3.87	-0.07	-3.00	-3.22	-3.47	-3.77	-3.96
41 Eri	B8.5 V	3.55	-0.11	-3.20	-3.43	-3.86	-4.27	-4.13
4622	B9 V	5.56	-0.06	-0.72	-0.85	-1.20	-1.61	-1.97
14 CVn	B9 V	5.15	-0.08	-1.31	-1.48	-1.78	-2.07	-2.29

the new E(B-V) and, hence, E(λ-V). The net effect is represented by the nearly horizontal dashed line.

If, on the other hand, the $(B-V)_o$ were precise but the ratio E(λ-V)/E(B-V) were incorrect by ±20% then the resultant correction, for E(B-V) = 0.20, is shown by the short vertical dashed line. The worst combined effect of the two influences is demonstrated by the solid arrows with the uncertainty in $(B-V)_o$ being the dominant factor.

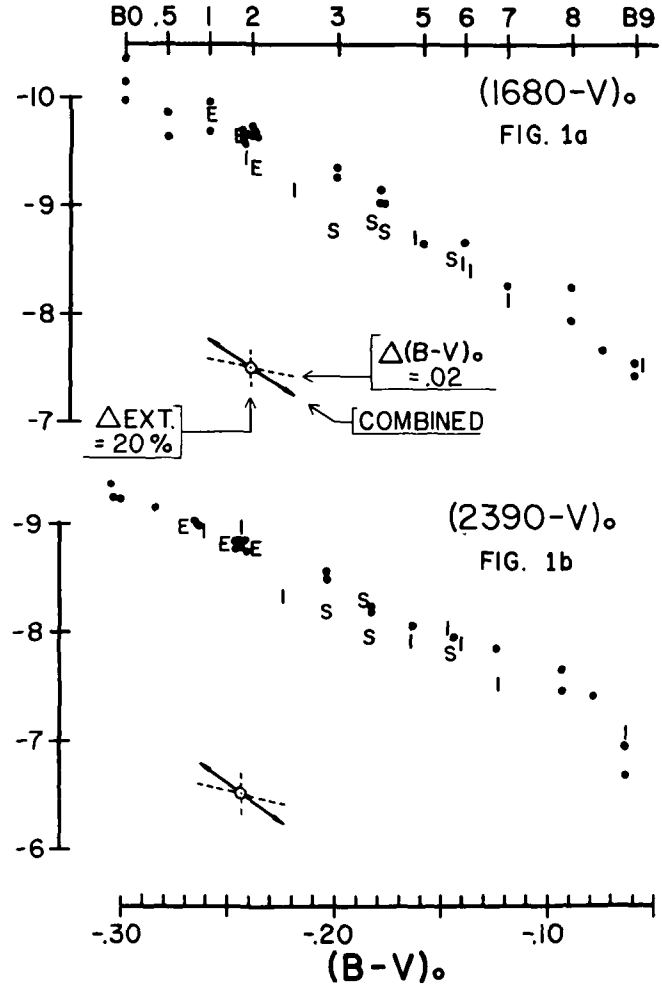

Figure 1a and 1b.—Color-color plots for the 25 standard stars and 15 program objects. Filled circles represent the standards; the letter "E", Be stars with no known shell or infrared excess; "S", shell stars with no known infrared excess; "I", any object with some degree of excess infrared flux. The graphs are of the color index $(\lambda-V)_o$ versus $(B-V)_o$, where, in (a), λ is the 1680 filter, in (b) it is the 2390 filter, and in (c), the 3320 filter.

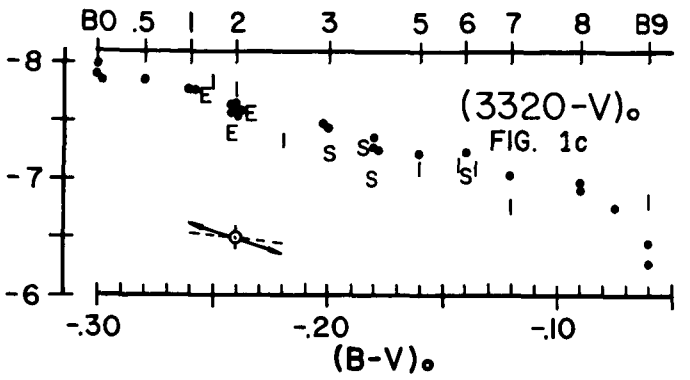

Figure 1c.

In order to graphically separate the potential effects of an infrared excess from a more conventional shell phenomenon and both of these from an even less complicated Be object, the program stars are plotted in a hierarchy of three symbols. If an object has an infrared excess to any noticeable degree it is plotted with an "I," regardless of any other characteristic. This scheme includes three shell stars at B1 (P Cyg), B5 (48 Lib) and B6 (κ Dra). The four remaining shell stars, either with a known lack or an unknown amount of infrared excess, are denoted with an "S." Emission objects with no known infrared excess are represented by an "E."

An examination of the figures reveals no significant difference between the program and comparison objects. Pushing "eyeball analysis" near its limits, one might conclude that there is a weak tendency for the program objects to lie below

Table 2

Coefficients for Approximate Linear Fit $(\lambda-V)_o = m(B-V)_o + b$		
λ	Slope, m	Intercept, b
1680	12.2	-6.77
2040	9.79	-6.86
2390	9.17	-6.58
2990	6.34	-6.50
3320	5.37	-6.36

the standard stars a couple of tenths in $(\lambda-V)_o$. However, if real, this is certainly not correlated with infrared excess since the three shell stars with a significant excess, mentioned above, are not leaders in this tendency. In fact, ε Cas is among the more deviant stars but Johnson's (1967) data show no unexpected infrared flux.

It is quite possible that a combination of observational error and "natural scatter," both in the stars and the reddening law, is at work here, with the apparent downward trend being an accidental bias due to the small sample size.

A slight, systematic underestimation of the reddening would produce a similar result. It is not impossible that an additional source of reddening is present in Be stars; witness, for example, the evidence for intrinsic polarization found by Coyne and Kruszewski(1969) and Serkowski (1970), which may be partly due to the presence of grains, and the fact that some Be stars do indeed exhibit an infrared excess. But, again, no correlation was found here between any ultraviolet deficiency and large infrared excesses.

Another possibility with a similar outcome would be slightly too-early classification. An object so categorized would be shifted to the left in Figures 1a, b and c, and, thus, would lie somewhat below the standard stars. However, the intercomparison of spectroscopic and Q-method spectral types mentioned earlier showed no such trend.

Figure 2 displays data from two ultraviolet filters in a slightly different manner. Here the spectral type-$(B-V)_o$ relationship does not fix the horizontal location of an object, although it retains an influence via the reddening-correction procedure. But, since there are fairly well-defined relationships between $(B-V)_o$ and the $(\lambda-V)_o$ color differences, there is naturally also a clearly defined sequence of stars in this figure distinguished by spectral type. The arrow in the lower left corner indicates the corrections to be made if the extinction ratio $E(\lambda-V)/E(B-V)$ is in error by ±20%.

The tick marks at the top of the figure indicate the spread of standard stars with the same classification. The only two discrepancies here are a B8 standard shifting into the B7 region and a B8.5 object moving to B8 but this may be the result of their not being classified on a scheme completely consistent with the earlier objects. The program stars' positions generally agree with the MK intervals defined by the standard stars. Although four objects show up at about one sub-type later and one appears slightly earlier, this is only a minor inconsistency and does not indicate any systematic misclassification of shell stars.

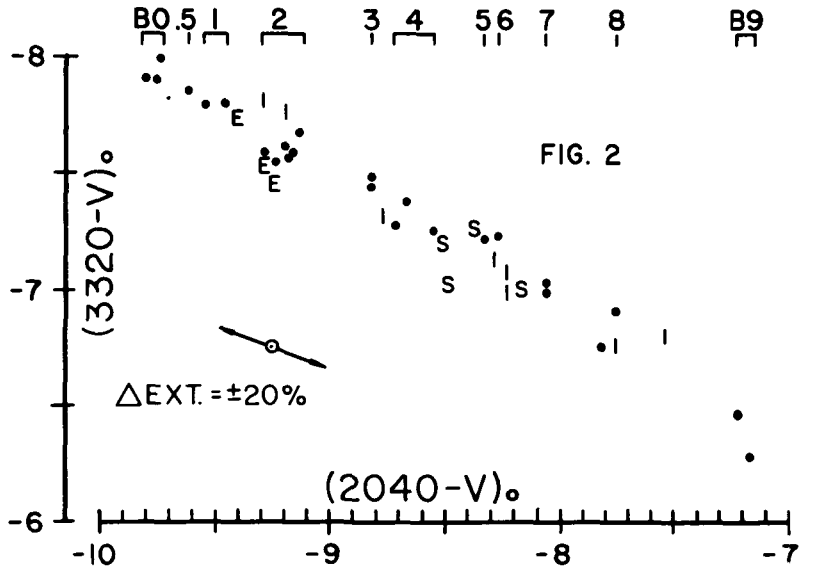

Figure 2.—A plot of the color differences $(3320-V)_o$ versus $(2040-V)_o$ with the ordering by spectral type indicated at the top. The arrows in the lower left area of the graph display the data point trajectories for a ±20 percent error in the interstellar extinction.

IV. SUMMARY

Examination of OAO photometry in the form of various color-color plots for some 40 B-type stars shows, not surprisingly, a smooth sequence of objects well-ordered by spectral type. Of specific interest was the behavior, in these plots, of a sub-set of 15 shell stars, Be stars and objects with some degree of infrared excess. No systematic difference was found that could be pointed to with confidence. A very slight tendency for the program objects to be dimmer in the ultraviolet filters is most likely due to either a modest underestimate of the reddening involved or an accidental bias caused by the small sample size.

The number of standard stars could usefully be increased and extended to earlier spectral types but the current file of shell stars with satisfactory photometry is nearly exhausted. Some scanner data does exist for an additional few shell stars. Another comparison that could be made in this same vein is one between the normal B stars and those with very high rotational velocities.

REFERENCES

Boone, J. C. 1970, Ph. D. thesis, University of Wisconsin.
Collins, G. W. and Harrington, J. P. 1966, Ap. J. 146, 152.
Coyne, G. V. and Kruszewski, A. 1969, A. J. 74, 528.
Geisel, S. L. 1970, Ap. J. (Letters), 161, L105.
Hiltner, W. A., Garrison, R. F. and Schild, R. E. 1969, Ap. J. 157, 313.
Huang, S.-S. 1969, Ap. J. 157, 835.
Johnson, H. L. 1958, Lowell Obs. Bull., No. 90, 4, 37.
_____ 1967, Ap. J. (Letters), 150, L39.
Lesh, J. R. 1968, Ap. J. Suppl. 17, 371.
Serkowski, K. 1970. Ap. J. 160, 1083.